

Development of an Autofluorescent Whole-Cell Biocatalyst by Displaying Dual Functional Moieties on *Escherichia coli* Cell Surfaces and Construction of a Coculture with Organophosphate-Mineralizing Activity^{∇†}

Chao Yang,^{1,2,‡} Yaran Zhu,^{1,2,‡} Jijian Yang,^{1,2} Zheng Liu,^{1,2} Chuanling Qiao,^{1*}
Ashok Mulchandani,^{3*} and Wilfred Chen³

State Key Laboratory of Integrated Management of Pest Insects & Rodents, Institute of Zoology, Chinese Academy of Sciences, Beijing 100101, China¹; Graduate School of the Chinese Academy of Sciences, Beijing 100049, China²; and Department of Chemical and Environmental Engineering, University of California, Riverside, California 92521³

Received 20 August 2008/Accepted 14 October 2008

Surface display of the active proteins on living cells has enormous potential in the degradation of numerous toxic compounds. Here, we report the codisplay of organophosphorus hydrolase (OPH) and enhanced green fluorescent protein (GFP) on the cell surface of *Escherichia coli* by use of the truncated ice nucleation protein (INPNC) and Lpp-OmpA fusion systems. The surface localization of both INPNC-OPH and Lpp-OmpA-GFP was demonstrated by Western blot analysis, immunofluorescence microscopy, and a protease accessibility experiment. Anchorage of GFP and OPH on the outer membrane neither inhibits cell growth nor affects cell viability, as shown by growth kinetics of cells and stability of resting cultures. The engineered *E. coli* can be applied in the form of a whole-cell biocatalyst and can be tracked by fluorescence during bioremediation. This strategy of codisplay should open a new dimension for the display of multiple functional moieties on the surface of a bacterial cell. Furthermore, a coculture comprised of the engineered *E. coli* and a natural *p*-nitrophenol (PNP) degrader, *Ochrobactrum* sp. strain LL-1, was assembled for complete mineralization of organophosphates (OPs) with a PNP substitution. The coculture degraded OPs as well as PNP rapidly. Therefore, the coculture with autofluorescent and mineralizing activities can potentially be applied for bioremediation of OP-contaminated sites.

Synthetic organophosphates (OPs) are widely used to control various pests for agriculture and for public health protection, and these account for ~38% of total pesticides used globally (38). Over 40 million kilograms of OP pesticides is used annually in the United States, with another 20 million kilograms produced for export (36). OPs are acute neurotoxins by virtue of their potent inhibition of acetylcholinesterase (16, 39).

Organophosphorus hydrolases (OPHs), which are capable of hydrolyzing a wide range of oxon and thion OPs, have been extensively studied (25, 34). Most microorganisms that produce OPH are gram-negative bacteria, and their OPH is located within the cells (38). Gram-negative bacteria possess a complex cell envelope structure that consists of a cytoplasmic membrane, cell wall, and outer membrane. The outer membrane prevents OPs from interacting with OPH residing within the cell, reducing the overall catalytic efficiency (28). This bot-

tleneck, however, could be eliminated if OPH is displayed on the cell surface (21, 28, 36). Various surface-anchoring motifs that possess the potential to cross both the cytoplasmic and outer membranes have been developed to target heterologous proteins onto the cell surface, such as the lipoprotein-outer membrane protein A chimera (Lpp-OmpA), ice nucleation protein (INP), and autotransporter (20, 32).

The Lpp-OmpA chimera consists of the signal sequence and the first nine N-terminal amino acids of the major *Escherichia coli* Lpp joined to a transmembrane domain (amino acids 46 to 159) from OmpA (8). The Lpp-OmpA-based cell display system has been extensively used for the display of heterologous proteins, such as β -lactamase (11), cellulases (12), the scFv antibody (6), cyclodextrin glucanotransferase (42), and chitin-binding domain (43), on the surface of *E. coli*.

The INP, which confers on host cells the ability to nucleate crystallization in supercooled water, is an outer membrane protein of *Pseudomonas syringae* (17, 44). The INP has a multidomain organization with an N-terminal domain containing three or four transmembrane spans, a C-terminal domain, and a highly repetitive central domain for ice nucleation (17, 44). The two types of the several identified INPs that have been used as anchoring motifs for display of foreign proteins on the cell surface are InaK from *P. syringae* KCTC1832 (15) and InaV from *P. syringae* INA5 (33).

p-Nitrophenol (PNP), produced from hydrolysis of OPs with a *p*-nitrophenyl substitution, is a stable and toxic intermediate and has been listed as a priority pollutant by the U.S. Envi-

* Corresponding author. Mailing address for Chuanling Qiao: State Key Laboratory of Integrated Management of Pest Insects & Rodents, Institute of Zoology, Chinese Academy of Sciences, Beijing 100101, China. Phone: 86-10-64807191. Fax: 86-10-64807099. E-mail: qiaocl@ioz.ac.cn. Mailing address for Ashok Mulchandani: Department of Chemical and Environmental Engineering, University of California, Riverside, CA 92521. Phone: (951) 827-6419. Fax: (951) 827-5696. E-mail: adani@engr.ucr.edu.

‡ C.Y. and Y.Z. contributed equally to this work.

† Supplemental material for this article may be found at <http://aem.asm.org/>.

[∇] Published ahead of print on 24 October 2008.

TABLE 1. Strains, plasmids, and primers used in this study

Strain, plasmid, or primer	Description ^a	Source or reference
<i>E. coli</i> strains		
XL1-Blue	<i>recA1 endA1 gyrA96 thi-1 hsdR17</i> (r _K ⁻ m _K ⁺) <i>supE44 relA1 lac</i> (F' <i>proAB lacI</i> ^q ZΔM15 Tn10 [Tet ^r])	Stratagene
DH5α	<i>supE44 ΔlacU169</i> (φ80 <i>lacZ</i> ΔM15) <i>recA1 endA1 hsdR17</i> (r _K ⁻ m _K ⁺) <i>thi-1 gyrA relA1 F⁻ Δ(lacZYA-argF)</i>	Tiangen
Plasmids		
pOP131	Gene source of Lpp-OmpA fusion	28
pEGFP-N3	Source of <i>gfp</i> gene	5
pUC18	Vector for construction of <i>lpp-ompA-gfp</i> fusion gene	TaKaRa
pLOG18	pUC18 derivative, vector for expressing Lpp-OmpA-GFP on the cell surface, <i>lac</i> promoter, Ap ^r	This study
pPNCO33	<i>E. coli/Pseudomonas</i> shuttle vector for expressing INPNC-OPH on the cell surface, <i>oriT</i> , RSF1010, <i>oriV</i> , <i>lacI</i> ^q , <i>tac</i> promoter, Km ^r	36
pUO18	pUC18 derivative, control plasmid for expressing OPH intracellularly	This study
pUG18	pUC18 derivative, control plasmid for expressing GFP intracellularly	This study
Primers		
P1	<u>GAATTCCTCTAGAGGGTATTAATAATGAAAGCTACTAAACTGGTA</u>	This study
P2	<u>GGATCCGTTGTCCGGACGAGTGCCGAT</u>	This study
P3	<u>GGATCCATGGTGAGCAAGGGC</u>	This study
P4	<u>CTGCAGTTACTTGTACAGCTCGTCCA</u>	This study
P5	<u>GAATTCATGCAAACGAGAAGG</u>	This study
P6	<u>GGATCCTCATGACGCCCGCAAGGT</u>	This study
P7	<u>GAATTCATGGTGAGCAAGGGC</u>	This study

^a The restriction sites in the primers (5[prime]→3[prime]) are underlined. Tet, tetracycline; Ap, ampicillin; Km, kanamycin.

ronmental Protection Agency (21). One strategy to avoid the generation of toxic hydrolytic products is to combine bacteria with complementary metabolic pathways into functional assemblages. This approach has been used for biodegradation of several xenobiotic pollutants, including 4-chlorodibenzofuran (1), parathion (13), and chlorpyrifos (46).

The green fluorescent protein (GFP) from the jellyfish *Aequorea victoria* can be expressed as a fluorescent protein in heterologous hosts without the need for specific cofactors or exogenous substrates (4) and can be detected noninvasively using fluorescence microscopy and flow cytometry (19). In field studies, GFP has been used as a marker to assess the fate and activity of specific degrading microorganisms (9, 10). Enhanced GFP, which is a red-shifted variant of GFP, assembles the chromophore more rapidly, shows much stronger fluorescence than wild-type GFP, and fluoresces after exposure to daylight (5, 27).

In this study, we aimed to construct autofluorescent whole-cell biocatalysts by coexpressing OPH and GFP on the *E. coli* cell surface. The engineered *E. coli* was endowed with high catalytic activity by overcoming the substrate uptake limitation, its fate and activity in the environment could be easily monitored by fluorescence. Furthermore, a coculture with OP-mineralizing activity was constructed by coculture of the engineered *E. coli* with a natural PNP degrader, *Ochrobactrum* sp. strain LL-1.

MATERIALS AND METHODS

Bacterial strains, plasmids, and culture conditions. *E. coli* XL1-Blue was used for codisplay of OPH and GFP. *E. coli* DH5α was used for recombinant DNA manipulation. *Ochrobactrum* sp. strain LL-1, a natural PNP degrader, grew in coculture with XL1-Blue for complete mineralization of OPs with a PNP substitution. Plasmids pOP131 (28) and pEGFP-N3 (5) were used as the source of

lpp-ompA and *gfp* genes, respectively. Plasmid pUC18 was used to construct the *lpp-ompA-gfp* fusion gene. Plasmid pPNCO33 (36) was used to target a truncated INP protein (INPNC)-OPH to the cell surface. The INPNC-OPH gene fragment was subcloned into EcoRI/HindIII-digested pVLT33 (7), a low-copy-number plasmid, to generate pPNCO33. All strains, plasmids, and primers used in this study are listed in Table 1.

E. coli strains bearing plasmids were grown in Luria-Bertani (LB) medium (31) supplemented with either ampicillin (100 μg/ml) or kanamycin (20 μg/ml). Expression of both INPNC-OPH and Lpp-OmpA-GFP was induced with 0.1 mM IPTG (isopropyl-β-D-thiogalactopyranoside) for 24 h at 25°C when cells were grown to an optical density at 600 nm (OD₆₀₀) of 0.5. *Ochrobactrum* sp. strain LL-1 was grown in minimal salt medium (18) with 0.2 mM PNP at 25°C.

Plasmid construction. The *lpp-ompA* fusion gene was PCR amplified from plasmid pOP131 using primers P1 and P2. The PCR products were digested with EcoRI and BamHI and then ligated into similarly digested pUC18 to generate pLO18. The *gfp* gene was PCR amplified from plasmid pEGFP-N3 using primers P3 and P4. The PCR products were digested with BamHI and PstI and then ligated into similarly digested pLO18 to generate pLOG18. To construct a control plasmid for the expression of the OPH intracellularly, the *opd* gene was PCR amplified from plasmid pPNCO33 using primers P5 and P6. The PCR product was digested with EcoRI and BamHI and then ligated into similarly digested pUC18 to generate pUO18. To construct a control plasmid for the expression of GFP intracellularly, the *gfp* gene was PCR amplified from plasmid pEGFP-N3 by using primers P7 and P4. The PCR product was digested with EcoRI and PstI and then ligated into similarly digested pUC18 to generate pUG18. The recombinant plasmids were sequenced to verify the correct sequence of the inserted genes. Transformation of plasmid into *E. coli* XL1-Blue was carried out using the CaCl₂ method (31).

Cell fractionation. Cells were harvested and resuspended in 25 mM Tris-HCl buffer (pH 8.0). The cell lysate was prepared as described below. Lysozyme was added to a final concentration of 50 μg/ml. The cells were incubated on ice for 1 h and then disrupted by sonication on ice in three pulses of 10 s each. The crude extract was centrifuged for 10 min at 11,000 × g to remove cell debris. The cell extract was then centrifuged for 1 h at 115,000 × g to separate the membrane and soluble fractions. The supernatant representing the soluble fraction was retained. For further outer membrane fractionation, the pellet (total membrane fraction) was resuspended with phosphate-buffered saline (PBS) (31) containing 0.01 mM MgCl₂ and 2% Triton X-100 for solubilization of the inner membrane and was

incubated for 30 min at room temperature, and then the outer membrane fraction was repelleted by ultracentrifugation (22).

Western blot analysis. Samples of the whole-cell lysates and soluble and outer membrane fractions were analyzed by sodium dodecyl sulfate-polyacrylamide gel electrophoresis with 10% (wt/vol) acrylamide (31). After electrophoresis, the separated proteins were electroblotted overnight at 40 V to the nitrocellulose membrane (Millipore, Billerica, MA) with a tank transfer system (Bio-Rad, Hercules, CA) containing a transfer buffer (25 mM Tris, 192 mM glycine, 10% methanol). After blocking nonspecific binding sites with 3% bovine serum albumin in TBST buffer (20 mM Tris-HCl, pH 7.5, 150 mM NaCl, 0.05% Tween-20), the membrane was incubated with either rabbit anti-GFP polyclonal antibody (Molecular Probes, Eugene, OR) or anti-OPH serum (36) at a 1:1,000 dilution in TBST buffer. Subsequently, the membrane was incubated with alkaline phosphatase-conjugated goat anti-rabbit immunoglobulin G (IgG) antibody (Promega, Madison, WI) at a 1:2,000 dilution. The membrane was then stained with Nitro Blue Tetrazolium-BCIP (5-bromo-4-chloro-3-indolylphosphate) in alkaline phosphatase buffer (100 mM Tris-HCl, pH 9.0, 100 mM NaCl) for visualization of antigen-antibody conjugates.

Immunofluorescence microscopy. Cells were harvested and resuspended ($OD_{600} = 0.5$) in PBS with 3% bovine serum albumin. Cells were then incubated with either anti-GFP antibody or OPH antisera at a 1:1,000 dilution for 2 h at 30°C. After being washed with PBS, the cells were resuspended in PBS with goat anti-rabbit IgG conjugated with rhodamine (Invitrogen, Mukilteo, WA) at a 1:500 dilution and were incubated for 1 h at 30°C. Prior to microscopic observation, cells were washed five times with PBS and mounted on poly-L-lysine-coated microscopic slides. Photographs were taken using fluorescence microscopy (Nikon) equipped with fluorescein isothiocyanate and rhodamine filters.

OPH assay. Cells were harvested and resuspended in 50 mM citrate-phosphate buffer with 50 μ M $CoCl_2$ (pH 8.0). The cell lysate was prepared as described above. For each assay, 200 μ l of cells ($OD_{600} = 1.0$) was added to 700 μ l of 50 mM citrate-phosphate buffer with 50 μ M $CoCl_2$ (pH 8.0) and 100 μ l of 20 mM paraoxon (Sigma) in 10% methanol. Changes in absorbance (410 nm) were measured with a Beckman DU800 spectrophotometer for 2 min at 37°C. Activities are expressed as units (micromoles of paraoxon hydrolyzed per minute) per OD_{600} of whole cells ($\epsilon_{410} = 16,500 M^{-1} cm^{-1}$ for PNP).

Measurement of whole-cell fluorescence. The GFP fluorescence intensity was determined using a fluorescence spectrophotometer (F-4500; Hitachi, Japan) with a bandwidth of 5 nm, an excitation wavelength of 488 nm, and an emission wavelength of 510 nm. Cells were diluted to an OD_{600} of 1.0 by using a PBS buffer (pH 7.5) before fluorescence was measured. The fluorescence signal of the untransformed cells diluted to an OD_{600} of 1.0 was set as the background level and was subtracted from the overall fluorescence.

Protease accessibility assay. Cells were harvested, suspended in a PBS buffer, and adjusted to an OD_{600} of 10. Pronase (4 units/mg; Sigma, St. Louis, MO) was added to a final concentration of 2 mg/ml. Cell suspensions were incubated at 37°C for 3 h. Subsequently, pronase-treated and untreated cells were assayed for OPH activity and GFP fluorescence as described above.

Stability study of resting cultures. Cells were grown in 50 ml of LB medium supplemented with 0.1 mM IPTG, 100 μ g/ml ampicillin, and 20 μ g/ml kanamycin for 2 days, washed twice with 50 ml of 150 mM NaCl solution, resuspended in 5 ml of 50 mM citrate-phosphate buffer with 50 μ M $CoCl_2$ (pH 8.0), and incubated in a shaker at 25°C. Over a 2-week period, 0.1 ml of samples was removed each day. Samples were centrifuged and resuspended in 0.1 ml of 50 mM citrate-phosphate buffer (pH 8.0) containing 50 μ M $CoCl_2$. OPH activity assays were conducted as described above.

Biodegradation of OPs by constructed coculture. A natural PNP degrader, *Ochrobactrum* sp. strain LL-1, was isolated from the sludge of a wastewater treatment plant. Details of the isolation, identification, and degradation characteristics of strain LL-1 are described in the supplemental material. For expression of INPNC-OPH, *E. coli* XL1-Blue/pLOG18/pPNCO33 cells were induced with IPTG as described above. Strain LL-1 was inoculated at an OD_{600} of 0.1 in minimal salt medium (18) with 0.2 mM PNP and incubated at 25°C on a shaker at 200 rpm until the yellow color of PNP disappeared. Subsequently, the induced XL1-Blue and LL-1 cells (1 g for each) were mixed, followed by two washes with 50 mM citrate-phosphate buffer (pH 8.0) and resuspension in the same buffer supplemented with 50 μ M $CoCl_2$. For the OP and PNP degradation experiments, 0.2 mM paraoxon, parathion, or methyl parathion was added to cell suspension. Samples were incubated at 25°C with shaking, taken out at different time points, and measured for the residual OP concentration and PNP released from the hydrolysis of OPs by gas chromatography and high-performance liquid chromatography, respectively (24, 47).

Nucleotide sequence accession number. The 16S rRNA gene sequence of strain LL-1 has been deposited in the GenBank database under accession no. EU098001.

RESULTS AND DISCUSSION

Regulated coexpression of OPH and GFP on the cell surface. Two different anchoring motifs were employed for the targeting of OPH and GFP onto the cell surface in order to minimize direct competition for the same translocation machinery. To date, only a few anchoring motifs, which include Lpp-OmpA from *E. coli* and INP from *P. syringae*, have been shown to target GFP to the cell surface (22, 35). Here, the Lpp-OmpA chimera, comprised of a localization domain (Lpp) and a transmembrane domain (OmpA), was employed as an anchoring motif, and a pUC18-based vector, pLOG18, was used to target Lpp-OmpA-GFP to the cell surface of *E. coli*. For the coexpression of OPH on the *E. coli* surface, we took advantage of an INP-derived anchoring motif, INPNC, and a compatible plasmid, pPNCO33 (36), which contains an RSF origin of replication, to target INPNC-OPH to the cell surface. Expression of INPNC-OPH is tightly regulated by a *tac* promoter due to the presence of the *lacI^q* gene on the plasmid. Both pPNCO33 and pLOG18 can coexist in the same cell because of the compatibility of the RSF origin of replication with the pUC origin of replication (7). Introduction of plasmids was carried out in a stepwise manner, and the resulting strain was named XL1-Blue/pLOG18/pPNCO33. The Lpp-OmpA and INP systems used in this study look promising, since they are well suited as a carrier of relatively large inserts. The largest proteins that have been successfully displayed with Lpp-OmpA and INP in *E. coli* so far are a 74-kDa cyclodextrin glucanotransferase and a 90-kDa chitinase, respectively (42, 45).

Production of the Lpp-OmpA-GFP fusion protein was verified by Western blotting with anti-GFP antibody. A specific band corresponding to Lpp-OmpA-GFP at 43 kDa was detected in whole-cell lysates (Fig. 1A, lane 5). However, no signal was detected with the control cells. The localization of Lpp-OmpA-GFP in the outer membrane fraction was also demonstrated by immunoblotting (Fig. 1A, lane 3). Expression of the INPNC-OPH fusion protein was probed by immunoblotting with OPH antisera, and the expected 82-kDa band was detected in both whole-cell lysates and outer membrane fractions (Fig. 1B, lanes 4 and 2, respectively). Over 70% of the OPH activity was detected in the membrane fraction. In parallel, more than 70% of the activity was present on the cell surface as judged from the ratio of whole-cell activity to cell lysate activity.

Protease accessibility experiments were performed to ascertain the surface localization of fusion proteins. GFP is resistant to many common proteases but not pronase, which is a mixture of broad-specificity proteases (2). Since pronase cannot readily penetrate the cell membrane, degradation should occur only with proteins exposed on the cell surface. With the pronase treatment, the fluorescence intensity for XL1-Blue/pLOG18/pPNCO33 cells decreased by 82%, while the fluorescence intensity of cells expressing GFP (pUG18) intracellularly dropped only 7%. Similarly, the OPH activity of XL1-Blue/pLOG18/pPNCO33 cells decreased by 84%, while the OPH activity of cells expressing OPH (pUO18) intracellularly

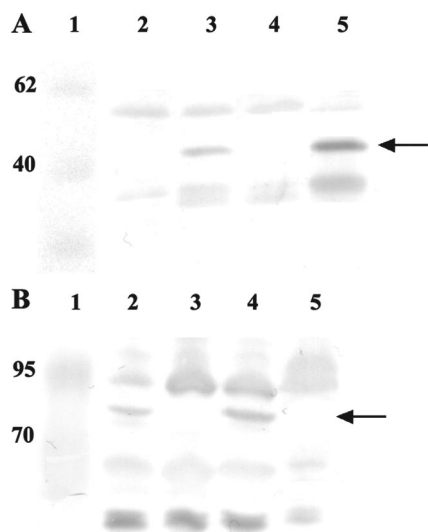


FIG. 1. Western blot analysis for subcellular localization of expressed Lpp-OmpA-GFP and INPNC-OPH fusion proteins in *E. coli* XL1-Blue/pLOG18/pPNCO33. Molecular weights (in thousands) are listed to the left of the lanes. (A) Western blot analysis of different cellular fractions with anti-GFP antibody. Lane 1, protein markers; lane 2, negative control (XL1-Blue/pUC18/pVLT33); lane 3, outer membrane fraction; lane 4, soluble fraction; lane 5, whole-cell lysates. The Lpp-OmpA-GFP fusion protein is indicated by an arrow. (B) Western blot analysis of different cellular fractions with anti-OPH serum. Lane 1, protein markers; lane 2, outer membrane fraction; lane 3, soluble fraction; lane 4, whole-cell lysates; lane 5, negative control (XL1-Blue/pUC18/pVLT33). The INPNC-OPH fusion protein is indicated by an arrow.

dropped only 6%. After the treatment of cells with pronase, the fractionated outer membrane was probed with either GFP or OPH antiserum. As expected, no signal corresponding to either of the two target proteins was detected in pronase-treated cells.

To confirm the presence of GFP and OPH on the cell surface, XL1-Blue cells were probed with either GFP or OPH antiserum and then fluorescently stained with rhodamine-labeled IgG antibody. Since antibodies cannot diffuse through the cell membrane, specific interactions between a target antigen and an antibody should occur only with proteins exposed on the cell surface. Under fluorescence microscopy, XL1-Blue/pLOG18/pPNCO33 cells were brightly fluorescent when labeled with both antisera (Fig. 2A and C), and cells emitted bright green fluorescence (data not shown), which indicated that GFP was anchored on the cell surface in an active form. However, XL1-Blue cells expressing either the GFP (pUG18) or OPH (pUO18) intracellularly were not immunolabeled with either of the two antibodies (Fig. 2B and D). From all of these results, we concluded that both GFP and OPH were codisplayed functionally on the cell surface.

Whole-cell activity and fluorescence. The whole-cell activity of *E. coli* XL1-Blue/pLOG18/pPNCO33 displaying OPH was sixfold higher than that of XL1-Blue/pUO18 expressing cytosolic OPH. The surface-exposed OPHs have free access to OPs, and this enhances whole-cell catalytic efficiency. The activity and fluorescence increased gradually after induction with 0.1 mM IPTG and reached maximums at 24 h (Table 2). In this

study, 25°C proved to be an optimum induction temperature, which produced the highest whole-cell OPH activity and significant fluorescence. The activity and fluorescence were not detected for cultures with induction at 37°C, and the cultures with induction at 30°C exhibited a low activity level (0.006 U/OD₆₀₀) and weak fluorescence (30% of that achieved at 25°C). These observations suggest that a low temperature may be favorable for the correct folding and proper translocation of proteins (3). The adverse effects of a high temperature on the surface expression of foreign proteins were reported previously (28, 35).

Since the OPH and GFP targeted toward the cell surface are competing for the same surface sites, it is important to use different strengths of promoter and to investigate the optimal levels of coexpression of GFP and OPH in order to achieve both significant fluorescence and a high level of whole-cell activity. Here, expression levels of INPNC-OPH and Lpp-OmpA-GFP are controlled by a moderately high level of *tac* promoter and a moderate level of *lac* promoter, respectively. Effects of different levels of induction on activity and fluorescence were studied. The expressed INPNC-OPH and Lpp-OmpA-GFP were located in the outer membrane fraction when IPTG induction was performed at a concentration of 0.1 mM (Fig. 3A and B). However, the fusion proteins produced with induction at higher IPTG concentrations (0.5 and 1 mM) were present only in the soluble fraction. A high transcription rate can block the translocation pathway of a secreted protein, as translocation is generally the limiting step (30). The inhibitory effects of overexpression on the translocation pathway have been well documented (22, 35). In this study, whole-cell activity reached a maximum at an IPTG concentration of 0.1 mM (Fig. 3C). Further induction resulted in a gradual decline in activity. Fluorescence increased with increasing concentrations of IPTG because it was minimally affected by the barrier effect of the cell membrane (Fig. 3D). Our results suggest that induction with 0.1 mM IPTG provides an optimal balance between whole-cell activity and fluorescence.

Stability of *E. coli* cultures displaying fusion proteins. Anchorage of foreign proteins on the outer membrane may result in instability of the outer membrane and growth inhibition of the cells (32). To test whether coexpression of the GFP and OPH on the cell surface inhibits cell growth, growth kinetics of XL1-Blue/pLOG18/pPNCO33 and XL1-Blue/pUC18/pVLT33 were compared. No growth inhibition was observed for cells coexpressing GFP and OPH on the surface. The XL1-Blue/pLOG18/pPNCO33 cells showed the same growth profile as the XL1-Blue/pUC18/pVLT33 cells (see Fig. S1 in the supplemental material). The two cultures reached the same final cell density after 48 h of incubation. To monitor the stability of suspended cultures, whole-cell activity was determined periodically over a 2-week period. As shown in Fig. 4, whole-cell activity of XL1-Blue/pLOG18/pPNCO33 remained at essentially the original level over the 2-week period.

Biodegradation of OPs by constructed coculture. Complete mineralization of parathion or chlorpyrifos has been achieved by coculture of two genetically engineered strains (13) or two natural degraders (46), respectively. In this study, a coculture comprised of two metabolically complementary bacteria, *E. coli* XL1-Blue with OPH activity and *Ochrobactrum* sp. strain LL-1 with PNP-mineralizing capability, was assembled for

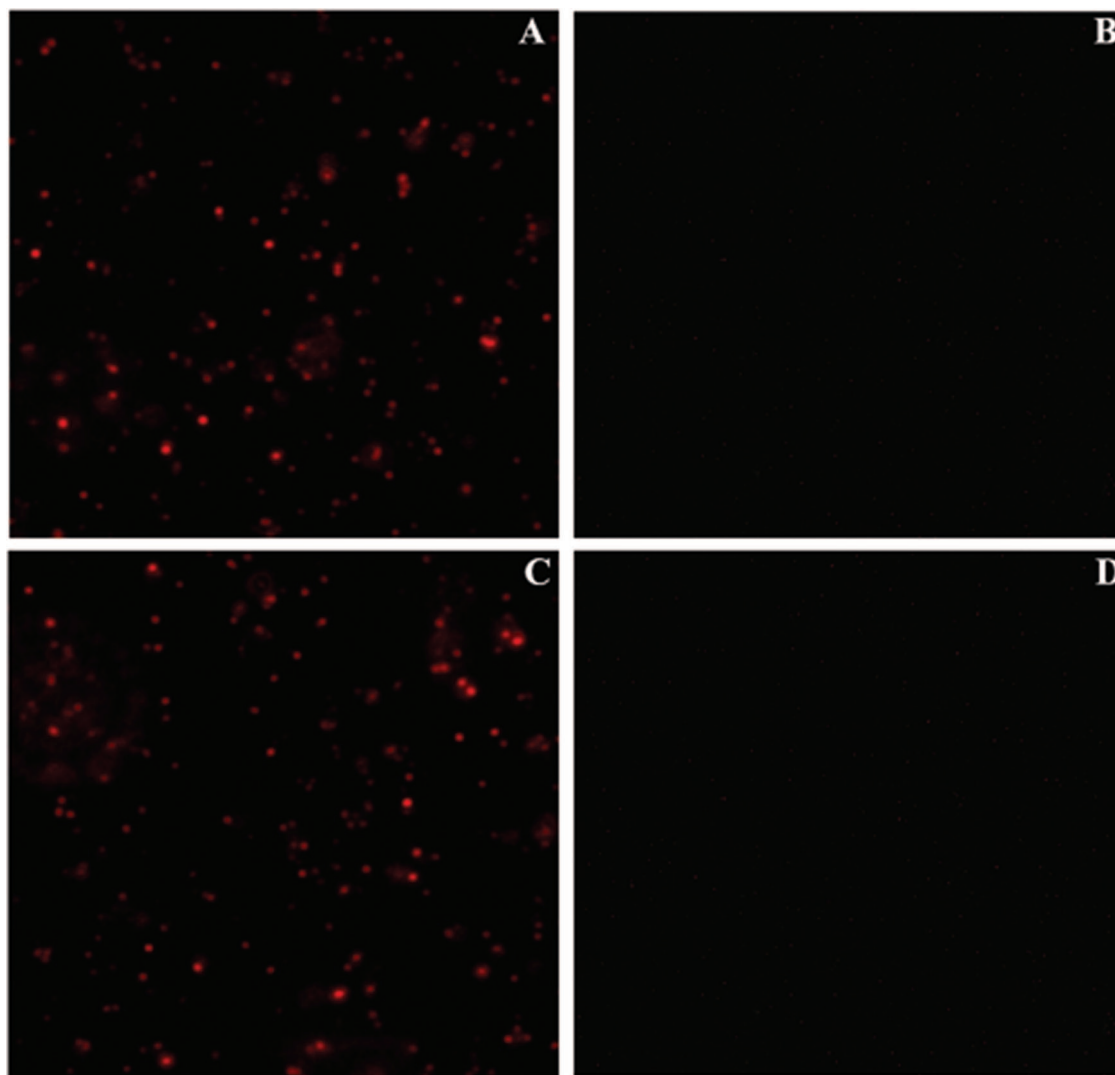


FIG. 2. Immunofluorescence micrographs of *E. coli* XL1-Blue/pLOG18/pPNCO33 (A and C), XL1-Blue/pUG18 (B), and XL1-Blue/pUO18 (D). Cells were probed with either rabbit anti-GFP antibody (A and B) or anti-OPH serum (C and D) and then fluorescently stained with goat anti-rabbit IgG–rhodamine conjugate.

complete mineralization of OPs with a PNP substitution. Strain LL-1 could utilize PNP as the sole carbon, nitrogen, and energy source. PNP (0.8 mM) was completely degraded by strain LL-1 in 28 h, concomitant with bacterial growth and nitrite

release (see Fig. S2 in the supplemental material). PNP degradation by strain LL-1 was very rapid at temperatures ranging from 18 to 30°C and at pHs ranging from 7.0 to 9.0, and the highest degradation rate was observed at 28°C and pH 8.0.

As shown in Fig. 5, paraoxon (0.2 mM) was quickly degraded within 60 min, with almost stoichiometric release of PNP. The PNP produced from hydrolysis of paraoxon was completely degraded within 2.5 h. Complete hydrolysis of parathion and methyl parathion occurred within 200 and 450 min, respectively (data not shown). The PNP produced from hydrolysis was completely degraded within 5.5 and 8 h for parathion and methyl parathion, respectively. These results suggest that the constructed coculture can function cooperatively to perform complete mineralization of OPs with a PNP substitution.

OPs with a PNP substitution (e.g., paraoxon, parathion, and methyl parathion) are hydrolyzed by OPH-displaying XL1-Blue to PNP, which is degraded by bacteria through formation of 4-nitrocatechol, 1,2,4-benzenetriol, or hydroquinone (14,

TABLE 2. Whole-cell OPH activity and GFP fluorescence assay^a

Time postinduction (h)	OPH activity (U/OD ₆₀₀)	Fluorescence intensity
0	ND	43 ± 5
6	0.012 ± 0.0021	621 ± 16
12	0.026 ± 0.0023	916 ± 21
18	0.031 ± 0.0035	1,028 ± 36
24	0.033 ± 0.0028	1,039 ± 28

^a *E. coli* XL1-Blue/pLOG18/pPNCO33 cells were incubated at 25°C for 24 h after induction with 0.1 mM IPTG. Samples were taken out at different time points and measured for whole-cell OPH activity and GFP fluorescence. Data are mean values ± standard deviations from three replicates. ND, not detected.

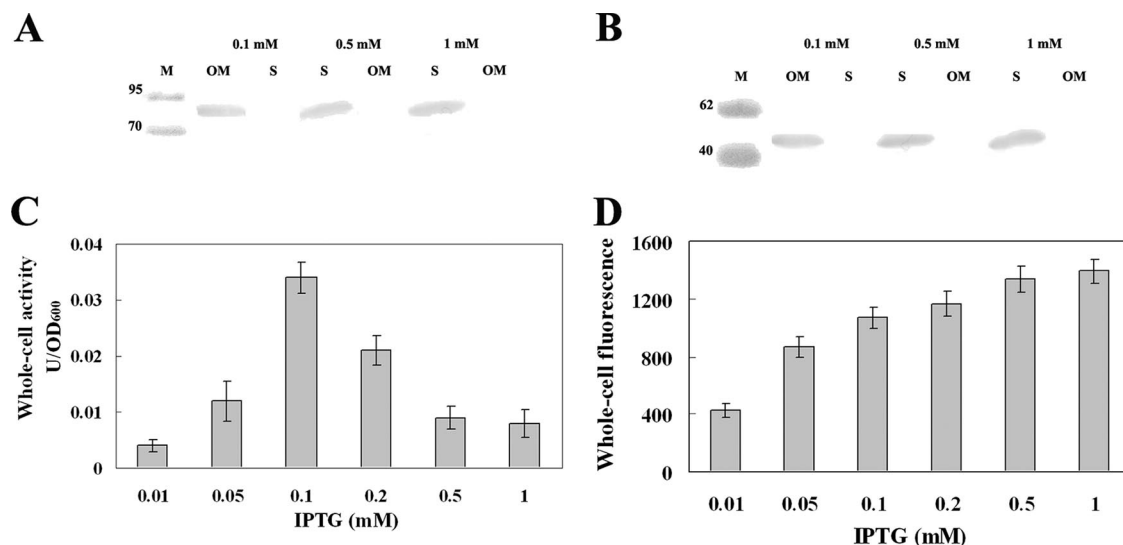


FIG. 3. Localization of the expressed INPNC-OPH (A) and Lpp-OmpA-GFP (B) in *E. coli* XL1-Blue at increasing concentrations of IPTG. The fusion proteins in the soluble fraction (S) and outer membrane fraction (OM) were probed with either anti-OPH serum or anti-GFP antibody. Molecular weights (in thousands) are listed to the left of the lanes. Whole-cell OPH activity (C) and fluorescence (D) of XL1-Blue/pLOG18/pPNCO33 under different levels of induction are shown. The activity was assayed with paraoxon as the substrate. Data are mean values \pm standard deviations from three replicates.

40). Both 4-nitrocatechol and 1,2,4-benzenetriol are the major degradation products of PNP in gram-positive bacteria (14), and hydroquinone is the key catabolic intermediate of PNP in gram-negative bacteria (40). During the degradation of PNP by strain LL-1, a chromatography peak with a retention time of 22.08 min appeared in gas chromatography-mass spectrometry analysis and was identified as hydroquinone by its mass-spectral properties (data not shown). However, no other putative intermediates (4-nitrocatechol or 1,2,4-benzenetriol) were detected. In addition, strain LL-1 was able to utilize 0.8 mM hydroquinone as the sole carbon source. In conclusion, OPs with a PNP substitution, like paraoxon, could be degraded by engineered XL1-Blue-natural LL-1 via degradation of paraoxon into PNP, which is further degraded into hydroquinone, which eventually leads to the tricarboxylic acid cycle (see Fig. S3 in the supplemental material).

Potential of coculture for bioremediation of OPs. Bioremediation is now accepted as a safe and economical alternative to physicochemical methods that are expensive and less efficient.

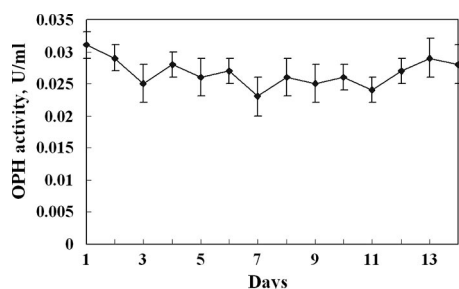


FIG. 4. Whole-cell OPH activity in suspended *E. coli* XL1-Blue cultures coexpressing OPH and GFP on the cell surface. The activity was assayed with paraoxon as the substrate. Data are mean values \pm standard deviations from three replicates.

At the present, several chemicals have been successfully removed from contaminated sites by inoculation of degrading consortium (26, 37). *E. coli*, which is very well known in regard to its genetic background, is still the most commonly used host for recombinant protein expression. Recombinant *E. coli* strains overexpressing atrazine chlorohydrolase have been applied for the remediation of atrazine-contaminated soil (41). However, more-effective and more-competitive strains that adapt well to the fluctuating environmental conditions and competition from indigenous microbial populations are required for in situ bioremediation of contaminated sites.

Bacteria with strong biofilm-forming capabilities have attracted much attention in biodegradation of pollutants. It has been found that some of these bacteria coaggregate with other microorganisms to develop biofilms and that these biofilms are capable of holding other microorganisms (29). In this study, we have demonstrated that strain LL-1 possesses strong biofilm-forming capability and is able to form biofilms together with *E.*

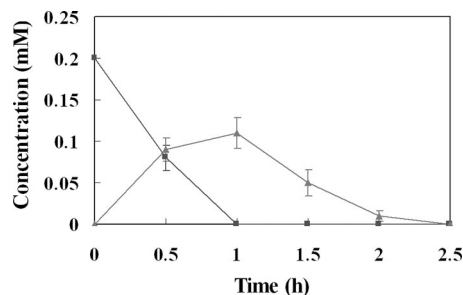


FIG. 5. Biodegradation of paraoxon by constructed coculture consisting of an OPH-displaying *E. coli* XL1-Blue and a natural PNP-degrading *Ochrobactrum* sp. LL-1 strain. Symbols: ■, paraoxon; ▲, PNP formed during the hydrolysis of paraoxon. Data are mean values \pm standard deviations from three replicates.

coli XL1-Blue as a coculture. The biofilm biomass formed by the coculture was larger than that formed by strain LL-1 alone (see Fig. S4 in the supplemental material). Strain LL-1 and *E. coli* XL1-Blue could be cultivated together in a biofilm, which may be beneficial for the long-term survival of coculture, as reported by Gilbert et al. (13) and by Liu and Li (23). We are currently investigating the degradation of organophosphorus compounds in a bioreactor with the constructed coculture.

ACKNOWLEDGMENTS

This work was financially supported by the 863 Hi-Tech Research and Development Program of the People's Republic of China (grant no. 2007AA06Z335) and the Innovation Program of the Chinese Academy of Sciences (grant no. KSCX2-YW-G-008).

REFERENCES

- Arfmann, H. A., K. N. Timmis, and R. M. Wittich. 1997. Mineralization of 4-chlorodibenzofuran by a consortium consisting of *Sphingomonas* sp. strain RW1 and *Burkholderia* sp. strain JWS. *Appl. Environ. Microbiol.* **63**:3458–3462.
- Bokman, S. H., and W. W. Ward. 1981. Renaturation of *Aequorea* green fluorescent protein. *Biochem. Biophys. Res. Commun.* **101**:1372–1380.
- Bukau, B. 1993. Regulation of the *Escherichia coli* heat-shock response. *Mol. Microbiol.* **9**:671–680.
- Chalfie, M., Y. Tu, G. Euskirchen, W. W. Ward, and D. C. Prasher. 1994. Green fluorescent protein as a marker for gene expression. *Science* **263**:802–805.
- Cormack, B. P., R. H. Valdivia, and S. Falkow. 1996. FACS-optimized mutants of the green fluorescent protein (GFP). *Gene* **173**:33–38.
- Daugherty, P. S., G. Chen, M. J. Olsen, B. L. Iverson, and G. Georgiou. 1998. Antibody affinity maturation using bacterial surface display. *Protein Eng.* **11**:825–832.
- de Lorenzo, V., L. Eltis, B. Kessler, and K. N. Timmis. 1993. Analysis of *Pseudomonas* gene products using *lacI^q/P_{trp}-lac* plasmids and transposons that confer conditional phenotypes. *Gene* **123**:17–24.
- Earhart, C. F. 2000. Use of an Lpp-OmpA fusion vehicle for bacterial surface display. *Methods Enzymol.* **326**:506–516.
- Elvång, A. M., K. Westerberg, C. Jernberg, and J. K. Jansson. 2001. Use of green fluorescent protein and luciferase biomarkers to monitor survival and activity of *Arthrobacter chlorophenolicus* A6 cells during degradation of 4-chlorophenol in soil. *Environ. Microbiol.* **3**:32–42.
- Errampalli, D., K. Leung, M. B. Cassidy, M. Kostrzynska, M. Blears, H. Lee, and J. T. Trevors. 1999. Applications of the green fluorescent protein as a molecular marker in environmental microorganisms. *J. Microbiol. Methods* **35**:187–199.
- Francisco, J. A., C. F. Earhart, and G. Georgiou. 1992. Transport and anchoring of β -lactamase to the external surface of *Escherichia coli*. *Proc. Natl. Acad. Sci. USA* **89**:2713–2717.
- Francisco, J. A., C. Stathopoulos, R. A. J. Warren, D. G. Kilburn, and G. Georgiou. 1993. Specific adhesion and hydrolysis of cellulose by intact *Escherichia coli* expressing surface anchored cellulose or cellulose binding domain. *Bio/Technology* **11**:491–495.
- Gilbert, E. S., A. W. Walker, and J. D. Keasling. 2003. A constructed microbial consortium for biodegradation of the organophosphorus insecticide parathion. *Appl. Microbiol. Biotechnol.* **61**:77–81.
- Jain, R. K., J. H. Dreisbach, and J. C. Spain. 1994. Biodegradation of *p*-nitrophenol via 1,2,4-benzenetriol by an *Arthrobacter* sp. *Appl. Environ. Microbiol.* **60**:3030–3032.
- Jung, H. C., J. M. Lebeault, and J. G. Pan. 1998. Surface display of *Zymomonas mobilis* levansucrase by using the ice-nucleation protein of *Pseudomonas syringae*. *Nat. Biotechnol.* **16**:576–580.
- Karalliedde, L., and N. Senanayake. 1999. Organophosphorus insecticide poisoning. *J. Int. Fed. Clin. Chem.* **11**:4–9.
- Kozloff, L. M., M. A. Turner, and F. Arellano. 1991. Formation of bacterial membrane ice-nucleation lipoglycoprotein complexes. *J. Bacteriol.* **173**:6528–6536.
- Kulkarni, M., and A. Chaudhari. 2006. Biodegradation of *p*-nitrophenol by *P. putida*. *Bioresour. Technol.* **97**:982–988.
- Larrainzar, E., F. O'Gara, and J. P. Morrissey. 2005. Applications of autofluorescent proteins for *in situ* studies in microbial ecology. *Annu. Rev. Microbiol.* **59**:257–277.
- Lee, S. Y., H. C. Jong, and X. Zhaohui. 2003. Microbial cell-surface display. *Trends Biotechnol.* **21**:45–52.
- Lei, Y., A. Mulchandani, and W. Chen. 2005. Improved degradation of organophosphorus nerve agents and *p*-nitrophenol by *Pseudomonas putida* JS444 with surface-expressed organophosphorus hydrolase. *Biotechnol. Prog.* **21**:678–681.
- Li, L., D. G. Kang, and H. J. Cha. 2004. Functional display of foreign protein on surface of *Escherichia coli* using N-terminal domain of ice nucleation protein. *Biotechnol. Bioeng.* **85**:214–221.
- Liu, Y., and J. Li. 2008. Role of *Pseudomonas aeruginosa* biofilm in the initial adhesion, growth and detachment of *Escherichia coli* in porous media. *Environ. Sci. Technol.* **42**:443–449.
- Liu, Z., C. Yang, and C. Qiao. 2007. Biodegradation of *p*-nitrophenol and 4-chlorophenol by *Stenotrophomonas* sp. *FEMS Microbiol. Lett.* **277**:150–156.
- Mulbry, W. W., J. F. Hams, P. C. Kearney, J. O. Nelson, C. S. McDaniel, and J. R. Wild. 1986. Identification of a plasmid-borne parathion hydrolase gene from *Flavobacterium* sp. by Southern hybridization with *opd* from *Pseudomonas diminuta*. *Appl. Environ. Microbiol.* **51**:926–930.
- Mulbry, W. W., E. Ahrens, and J. S. Karns. 1998. Use of a field-scale bioreactor for the degradation of the organophosphate insecticide coumaphos in cattle dip wastes. *Pestic. Sci.* **52**:268–274.
- Patterson, G. H., S. M. Knobel, W. D. Sharif, S. R. Kain, and D. W. Piston. 1997. Use of the green fluorescent protein and its mutants in quantitative fluorescence microscopy. *Biophys. J.* **73**:2782–2790.
- Richins, R. D., I. Kaneva, A. Mulchandani, and W. Chen. 1997. Biodegradation of organophosphorus pesticides by surface-expressed organophosphorus hydrolase. *Nat. Biotechnol.* **15**:984–987.
- Rickard, A. H., S. A. Leach, L. S. Hall, C. M. Buswell, N. J. High, and P. S. Handley. 2002. Phylogenetic relationships and coaggregation ability of freshwater biofilm bacteria. *Appl. Environ. Microbiol.* **68**:3644–3650.
- Rodrigue, A., A. Chanal, K. Beck, M. Muller, and L. Wu. 1999. Co-translocation of a periplasmic enzyme complex by a hitchhiker mechanism through the bacterial Tat pathway. *J. Biol. Chem.* **274**:13223–13228.
- Sambrook, J., and D. W. Russell. 2001. *Molecular cloning: a laboratory manual*, 3rd ed. Cold Spring Harbor Laboratory Press, Cold Spring Harbor, NY.
- Samuelson, P., E. Gunneriusson, P. A. Nygren, and S. Stahl. 2002. Display of proteins on bacteria. *J. Biotechnol.* **96**:129–154.
- Schmid, D., D. Pridmore, G. Capitani, R. Battistuta, J. R. Nesser, and A. Jann. 1997. Molecular organization of the ice nucleation protein InaV from *Pseudomonas syringae*. *FEBS Lett.* **414**:590–594.
- Serdar, C. M., and D. T. Gibson. 1985. Enzymatic hydrolysis of organophosphates: cloning and expression of a parathion hydrolase gene from *Pseudomonas diminuta*. *Bio/Technology* **3**:567–571.
- Shi, H., and W. W. Su. 2001. Display of green fluorescent protein on *Escherichia coli* cell surface. *Enzyme Microb. Technol.* **28**:25–34.
- Shimazu, M., A. Mulchandani, and W. Chen. 2001. Simultaneous degradation of organophosphorus pesticides and *p*-nitrophenol by a genetically engineered *Moraxella* sp. with surface-expressed organophosphorus hydrolase. *Biotechnol. Bioeng.* **76**:318–324.
- Singh, B. K., A. Walker, J. A. W. Morgan, and D. J. Wright. 2004. Biodegradation of chlorpyrifos by *Enterobacter* strain B-14 and its use in bioremediation of contaminated soils. *Appl. Environ. Microbiol.* **70**:4855–4863.
- Singh, B. K., and A. Walker. 2006. Microbial degradation of organophosphorus compounds. *FEMS Microbiol. Rev.* **30**:428–471.
- Sogorb, M. A., E. Vilanova, and V. Carrera. 2004. Future application of phosphotriesterases in the prophylaxis and treatment of organophosphorus insecticide and nerve agent poisoning. *Toxicol. Lett.* **151**:219–233.
- Spain, J. C., and D. T. Gibson. 1991. Pathway for biodegradation of *para*-nitrophenol in a *Moraxella* sp. *Appl. Environ. Microbiol.* **57**:812–819.
- Strong, L. C., H. McTavish, M. J. Sadowsky, and L. P. Wackett. 2000. Field-scale remediation of atrazine-contaminated soil using recombinant *Escherichia coli* expressing atrazine chlorohydrolase. *Environ. Microbiol.* **2**:91–98.
- Wan, H. M., B. Y. Chang, and S. C. Lin. 2002. Anchorage of cyclodextrin glucanotransferase on the outer membrane of *Escherichia coli*. *Biotechnol. Bioeng.* **79**:457–464.
- Wang, J. Y., and Y. P. Chao. 2006. Immobilization of cells with surface-displayed chitin-binding domain. *Appl. Environ. Microbiol.* **72**:927–931.
- Wolber, P. K. 1993. Bacterial ice nucleation. *Adv. Microb. Physiol.* **34**:203–237.
- Wu, M. L., C. Y. Tsai, and T. H. Chen. 2006. Cell surface display of Chi92 on *Escherichia coli* using ice nucleation protein for improved catalytic and antifungal activity. *FEMS Microbiol. Lett.* **256**:119–125.
- Xu, G., Y. Li, W. Zheng, X. Peng, W. Li, and Y. Yan. 2007. Mineralization of chlorpyrifos by co-culture of *Serratia* and *Trichosporon* spp. *Biotechnol. Lett.* **29**:1469–1473.
- Yang, C., N. Liu, X. Guo, and C. Qiao. 2006. Cloning of *mpd* gene from a chlorpyrifos-degrading bacterium and use of this strain in bioremediation of contaminated soil. *FEMS Microbiol. Lett.* **265**:118–125.